Banded iron formation to iron ore: A record of the evolution of Earth environments?

K.A. Evans[1], T.C. McCuaig[2], D. Leach[2], T. Angerer[2], and S.G. Hagemann[2]
[1]Department of Applied Geology, Curtin University, GPO Box U1987, WA 6845, Australia
[2]Australian Research Council Centre of Excellence for Core to Crust Fluid Systems, Centre for Exploration Targeting, School of Earth and Environment, The University of Western Australia, Crawley, Perth, WA 6009, Australia

ABSTRACT

Banded iron formations (BIF) are the protolith to most of the world's largest iron ore deposits. Previous hypogene genetic models for Paleoproterozoic "Lake Superior" BIF-hosted deposits invoke upwards, down-temperature flow of basinal brines via complex silica and carbonate precipitation/dissolution processes. Such models are challenged by the necessary SiO_2 removal. Thermodynamic and mass balance constraints are used to refine conceptual models of the formation of BIF-hosted iron ore. These constraints, plus existing isotope and halogen ratio evidence, are consistent with removal of silica by down- or up-directed infiltration of high-pH hypersaline brines, with or without a contribution from basinal brines. The proposed link to surface environments suggest that Paleoproterozoic BIF-ore upgrade may provide a record of a critical time in the evolution of the Earth's biosphere and hydrosphere.

INTRODUCTION

Banded iron formations (BIFs) record changing environmental conditions and are a precursor to the world's largest iron ore deposits. Vast volumes of BIFs were deposited on passive margins from ca. 2.6 Ga to the Great Oxygenation Event (GOE) at ca. 2.4 Ga (e.g., Beukes and Gutzmer, 2008). After 1.85 Ga, formation of iron formations essentially ceased until a restricted resurgence in the late Neoproterozoic (Young, 1976; Klein and Beukes, 1993) and more recent minor occurrences.

The temporal distribution of BIFs records a complex interplay between a cooling Earth and changes in mantle plume events, continental growth and tectonics, evolution of the biosphere and an increased flux of iron to the hydrosphere, which in turn had a fundamental control on the oxygen contents of the hydrosphere and redox state of the oceans (Isley and Abbott, 1999; Holland, 2005; Bekker et al., 2010). In most giant Paleoproterozoic BIF-hosted iron ore deposits (~35 wt% Fe) the formation of high-grade (>58 wt% Fe) iron ore from Lake Superior–type BIF is thought to have occurred post 2.2 Ga, after the GOE (Taylor et al., 2001; Rasmussen et al., 2007; Thorne et al., 2009), so the BIF-ore upgrade provides a record of the changing chemistry of the hydrosphere and atmosphere in the Paleoproterozoic.

In the Hamersley province, Western Australia, the BIF-ore upgrade is proposed to involve basinal brines, meteoric fluids, and supergene enrichment (e.g., Morris et al., 1980; Barley et al., 1999; Taylor et al., 2001; Thorne et al., 2004, 2008). Silica removal is proposed to occur by upward, down-temperature flow of basinal brines (e.g., Thorne et al., 2004; Gutzmer et al., 2006; Thorne et al., 2008), and it is this stage of the BIF-ore upgrade that is explored in this paper.

The challenge for models that involve removal of SiO_2 from BIF by down-temperature flow is that quartz solubility decreases with decreasing temperature (e.g., Manning, 1994), so fluid that moves down-temperature is a poor agent for quartz removal, unless large volumes of fluids enter the BIF in a silica-undersaturated state. Here, we combine numerical constraints with petrological, geochemical and isotopic characteristics of BIF-hosted iron ore from the Hamersley province, Western Australia, to constrain the conditions associated with silica loss and carbonate precipitation, and discuss the findings in the context of the temporal evolution of the world's atmosphere and oceans.

DEPOSIT SCALE PARAGENESIS

The mineralogy of BIF, hydrothermally altered BIF, and iron ore varies (e.g., Thorne et al., 2004; Rosiere et al., 2008; Mukhopadhyay et al., 2008; Angerer and Hagemann, 2010) but some features are sufficiently common to allow generalization. BIF protolith (Figs. 1A, 1B1, and 1B2) consists of magnetite- and chert-rich bands, iron silicates

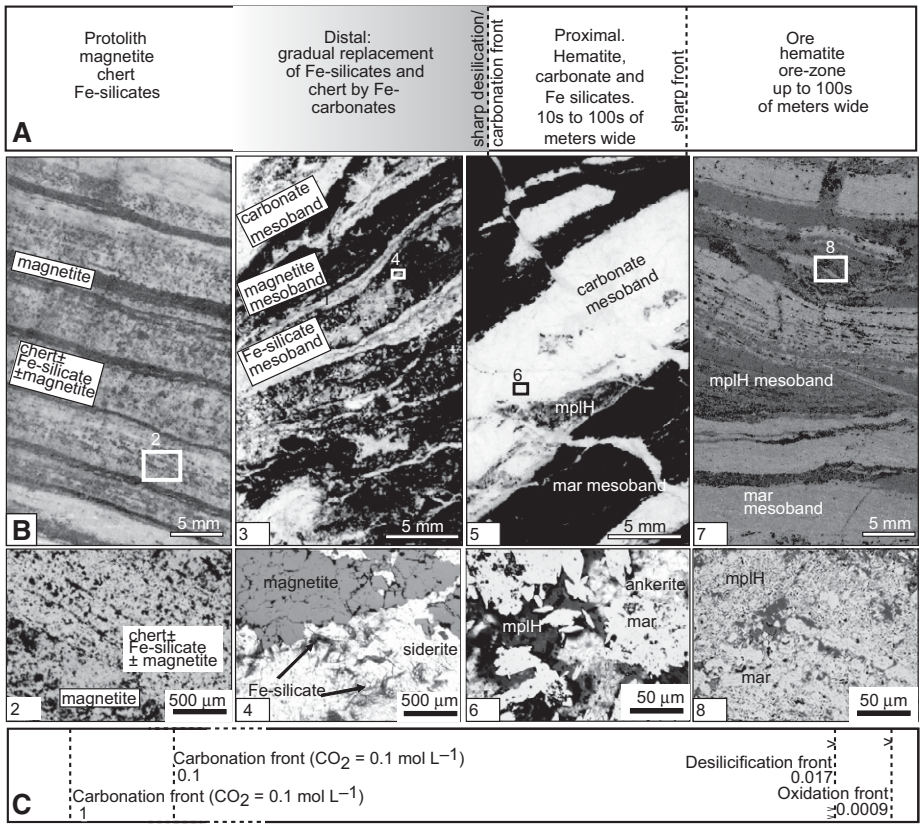

Figure 1. A: Commonly observed banded iron formation (BIF) alteration stages related to the formation of iron ore and their characteristics. B(b1–b8): Polished blocks and photomicrographs of the typical alteration stages. mplH—microplaty hematite; mar—martite. C: Results of mass balance calculations to determine the relative distances moved by decarbonation, desilicification and oxidation fronts. Values indicate distance traveled by front relative to the carbonation front for a solution with 1 mol L^{-1} CO_2.

GEOLOGY, February 2013; v. 41; no. 2; p. 99–102; Data Repository item 2013024 | doi:10.1130/G33244.1 | Published online 13 November 2012

± diagenetic carbonates. Initial hydrothermal alteration (Figs. 1A, 1B3, and 1B4), which may be gradational, involves conversion of some of the silicates to carbonates. Subsequently, chert and quartz are replaced by iron-bearing carbonate with, in some cases, conversion of magnetite to hematite, often with no apparent change in volume. Reaction fronts may be gradual (millimeter to decimeter scale) or knife-sharp on the scale of individual bands. Quartz may be precipitated locally in fault zones within shear veins (e.g., Hagemann et al., 1999; Thorne et al., 2010).

The carbonate-bearing alteration assemblage (Figs. 1A, 1B5, and 1B6) is separated from almost pure (hypogene) hematite iron ore (Figs. 1A, 1B7, and 1B8) by a sharp or gradational reaction front. Carbonate loss is thought to occur without iron mobility on a scale greater than a few cm (Taylor et al., 2001). Carbonate dissolution continues in the weathering environment.

Upgrade of BIF in the Hamersley province, Western Australia, is thought to have occurred from 2.15 Ga onwards during the waning stages of the Opthalmian orogeny (Rasmussen et al., 2007). There is evidence for extensional faulting and orogenic collapse at the proposed time of ore upgrade (Müller et al., 2005) and it has been suggested that topographic relief drove circulation of surface-derived waters through the fault system at this time (e.g., Hagemann et al., 1999; Oliver and Dickens, 1999).

Constraints on ore upgrade in the Hamersley are provided by fluid inclusion, isotopic, and halide concentration measurements. Fluid inclusions in carbonates are hypersaline, up to 24 wt% $CaCl_2$ equivalent, which were trapped at temperatures between 150 and 400 °C (Thorne et al., 2004; Brown et al., 2004), mainly at the lower end of this range. Quartz-hosted fluid inclusions (e.g., Brown et al., 2004) records periods of quartz growth, not quartz removal, so such inclusions may record either a different event, or a later stage of the silica dissolution event that is of interest here.

Iron oxide oxygen isotopes in unaltered BIF have $\delta^{18}O_{VSMOW}$ (Vienna Standard Mean Ocean Water) between 4‰ and 13‰, whereas hematite and magnetite in altered and mineralized rocks have $\delta^{18}O_{VSMOW}$ between −9‰ and −2.9‰ (Thorne et al., 2009). Carbon isotopes of carbonate minerals lie between −10‰ and 0‰, relative to Vienna Peedee belemnite (VPDB). The lower values are typical of unaltered BIF. Values in altered rocks could record equilbrium with either Paleoproterozoic ocean water or dolomite in the underlying Wittenoom Formation. Fluid inclusion Na/Br and Cl/Br ratios record overlapping populations of fluids: (1) seawater that has evaporated to halite saturation; and (2) meteoric waters that interacted with evaporites (Thorne et al., 2010).

CONSTRAINTS ON SILICA REMOVAL AND CARBONATE PRECIPITATION

Fluids in Equilibrium with BIF

Quartz solubility is sensitive to pressure, temperature (e.g., Manning, 1994), pH (Busey and Mesmer, 1977), and salinity (e.g., Shmulovich et al., 2006). Quartz and carbonate solubilities were calculated as a function of pressure, temperature and salt content (Fig. 2) using the methods outlined in the GSA Data Repository[1]. Calcite, rather than iron carbonate was used for the models because data for iron carbonates is sparse, but similar trends for iron carbonates are expected. Temperature is the first order control on quartz solubility, whereas calcite solubility depends strongly on pressure (Fig. 2A). Salinity-driven mineral precipitation/dissolution is minor for geothermal gradients <50 °C km^{-1} (Fig. 2B). There is no geothermal gradient for which silica dissolution is accompanied by carbonate precipitation in the observed quantities, so it is necessary to consider infiltration of out-of-equilibrium fluids.

Fluid out of Equilibrium with BIF

Infiltration of high-pH, out-of-equilibrium fluid can drive quartz removal via up- or down-temperature flow, because quartz is 4 orders of magnitude more soluble at pH 9 than it is at pH 6 (Busey and Mesmer, 1977). The desilicification/carbonation and oxidation fronts observed in BIFs are sufficiently sharp that they can be treated as advective chromatographic fronts; broadening by diffusion, dispersion and kinetic broadening can be neglected. The ratio of the distance traveled by a fluid to that of associated reaction front is given by

$$\frac{d_{\text{fluid}}}{d_{\text{rock}}} = \frac{c_{\text{i,rock,final}} - c_{\text{i,rock,initial}}}{\theta\left(c_{\text{i,fluid,initial}} - c_{\text{i,fluid,final}}\right)}, \qquad (1)$$

(adapted from Evans et al., 2003). d is the position of the front relative to the infiltration horizon in meters, c_i is the concentration of the reactant of interest in moles m^{-3}, and θ is porosity.

Relative positions of carbonation, desilicification, and oxidation fronts were calculated using the values given in Table DR1 (in the Data Repository), which are based on the assumption of infiltration an out-of-equilibrium, pH 9, SiO_2-free, CO_2-rich, O_2-bearing fluid (O_2 at

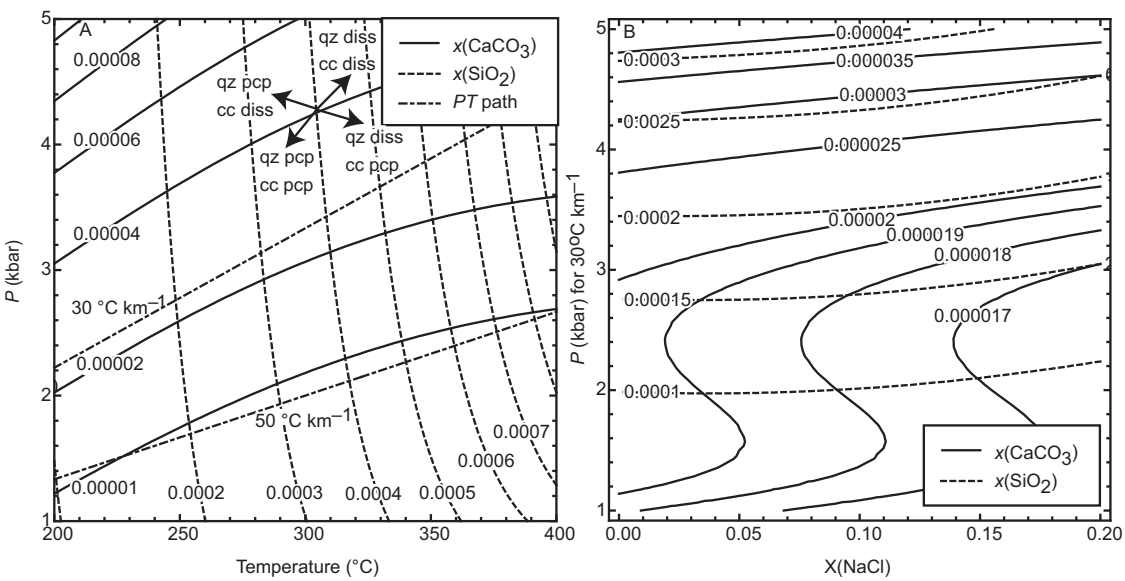

Figure 2. Results of thermodynamic calculations of SiO_2 and calcite solubility as a function of pressure and temperature (A), and temperature and salt concentration (B).

[1]GSA Data Repository item 2013024, information on the quartz solubility model and details of values used for calculations, is available online at www.geosociety.org/pubs/ft2013.htm, or on request from editing@geosociety.org or Documents Secretary, GSA, P.O. Box 9140, Boulder, CO 80301, USA.

10% of present-day values). Front positions were normalized to that of the most advanced carbonation front (Fig. 1B). The oxidation front is predicted to proceed the smallest distance, as observed, though the position of this front is modified by post-hypogene meteoric fluid and supergene processes. The carbonation front is predicted to advance further than the desilicification front for any reasonable combination of input parameters. In reality, the desilicification front coincides with a sharp increase in carbonate content, which suggests a reaction-induced porosity control on fluid infiltration.

Volumes of Fluid Flow

The relationship between time-integrated fluid flux and silica removal for hydrothermal alteration where pressure, temperature and fluid composition gradients are fixed, and for constant fluid flow rates is given by

$$Q = \frac{\Delta n_{SiO_2}}{\left(\frac{dc_{SiO_2}}{dl}\right)}, \qquad (2)$$

(c.f. Evans and Bickle, 1999, their equation 6). Q is the time-integrated fluid flux, in cubic meters of fluid per square meter of rock, Δn_{SiO_2} is the SiO_2 removed from the volume (moles m^{-3}), c_{SiO_2} is the concentration of SiO_2 in the fluid in (moles m^{-3}), and l is distance along the flow path (m). This expression is based on mass balance and can be applied to in- or out-of-equilibrium situations. Calculations were made for flow up- or down-temperature of a pH 9, silica-undersaturated fluid, such as might be derived from an ultramafic lithology or hypersaline evaporite-derived fluid. pH is assumed to drop from 9 to 5 during equilibration. dc_{SiO2}/dpH was calculated from Busey and Mesmer (1977) and checked against HCh output (Shvarov and Bastrakov, 1999).

Flow volumes were calculated for a single cubic meter of rock undergoing pH-driven quartz dissolution and scaled to estimate the volume needed to produce the observed SiO_2 depletion on a scale comparable to observed small iron ore deposits (3×10^8 m^3). The volume of fluid required is approximately ~10^9 m^3.

DISCUSSION AND CONCLUSIONS

The observed silica removal and carbonate precipitation needed for formation of a kilometer-scale BIF-hosted Fe deposit is inconsistent with in-equilibrium fluid flow (Fig. 2), but could be produced by pervasive infiltration of ~10^9 m^3 of a high pH (pH > 9) fluid flowing up- or down-temperature.

Density- or topography-driven infiltration (McLellan et al., 2004) of dense hypersaline brines evolved on continental margins (Fig. 3) provides a plausible source of high-pH fluid. The pH of hypersaline lakes today is up to 10, and the CO_2 content is high; reported alkalinities exceed 10,000 mg L^{-1} (Gosselin et al., 1994). These brines form on marginal platforms (Leach et al., 2010) and were present on the north Yilgarn margin in the Palaeoproterozoic (El Tabakh et al., 1999) and in Mesoproterozoic dolomitic argillites in the western United States (Gonzalez-Alvarez and Kerrich, 2011). The Yilgarn and Pilbara cratons may not have been adjacent at the time of ore formation, and the latitude of the Pilbara margin at that time is poorly known but existing constraints place the latitude within the range of those required for evaporite formation (Li, 2000). Fault zones in similar environments today are sufficiently permeable that proposed volumes could have flowed on a geologically reasonable timescale (Jones et al., 2002).

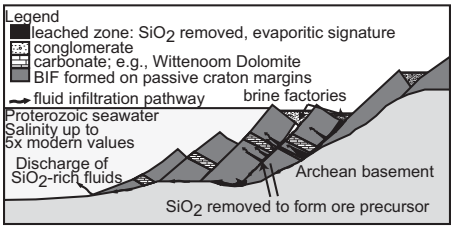

Figure 3. Proposed genetic model for desilicification of banded iron formation (BIF) by a density-driven, hypersaline, high-pH brine.

Carbon and oxygen isotopes of early carbonate and iron oxides in mineralized BIF are consistent with seawater derivation from Palaeoproterozoic seawater. High salinities and Na/Br and Cl/Br ratios record fluids typical of seawater that has evaporated to halite saturation (Thorne et al., 2010), which is also consistent with an involvement of evaporite-derived fluids. Temperatures of up to 250 °C are consistent with fluid inclusion evidence, and with other environments where voluminous quantities of surface-derived fluids infiltrate basement rocks (e.g., Gleeson and Yardley., 2003). However, temperatures >300 °C recorded by early assemblages at Mount Tom Price require a separate high-temperature alteration stage. SiO_2 deposition in outflow zones from the flow system described have not been recorded, to date, but may prove difficult to recognize given that chert was a common sedimentary rock at this time.

Some geometric constraints in mineralized Pilbara BIFs favour an upwards flowing fluid (e.g., Dalstra and Rosiere, 2004). The Wittenoom Formation underlies many of the ore-bearing units, and has been proposed as a way for basinal brines to access the BIF (e.g., Taylor et al., 2001). Dolomite in the Wittenoom Formation contains numerous shale bands (Davy, 1975), and is separated from the BIF by the Si-bearing Mount McRae shale and Sylvia Formation, so fluids from this unit would be at, or close to, SiO_2 saturation, unless fluids were focused solely within shale-free regions of the dolomite, such as the Paraburdoo Member (Thorne and Tyler, 1997). If this were the case then the dolomite in the Wittenoom Formation could have acted as an aquifer that supplied overlying iron formations with fluids derived either from faults that focused either down-flowing evaporitic brines with or without a contribution from upward-flowing basinal brines, as suggested by previous workers (e.g., Taylor et al., 2001).

Mafic and ultramafic rocks are present in the Pilbara (e.g., Barnes and Hoatson, 1994) and can equilibrate with water to provide high pH fluids, but such fluids are unlikely to have reached the BIF without interacting with Si-bearing rocks such as the Mount McRae shale.

Oxidized, sulfur-bearing, hypersaline brines produced on basin margins since 2.0 Ga have been linked to base metal sulfide deposition, including MVT (Mississippi Valley type) and SEDEX-Pb-Zn deposits (Leach et al., 2010). Such deposits older than 2.02 Ga have not been found; Archaean and Paleoproterozoic oceans were reduced and largely sulfur-depleted (e.g., Farquhar et al., 2010), so marginal hypersaline brines at 2.2 Ga, at the time of ore upgrade, could have had a significantly different composition to those today. It is interesting to speculate whether redox controls related to mobilization, transport, and deposition of Pb and Zn by Palaeoproterozoic evaporite-derived brines, such as a lack of sulfur (Leach et al., 2010) lack of oxidized source rocks and aquifers, or reduction of sulfate via rock-buffering in the immediate sub-surface, may have prevented formation of these deposit types prior to 2.02 Ga.

ACKNOWLEDGMENTS

We thank Rob Kerrich, Hilke Dalstra, and an anonymous reviewer for perceptive, knowledgeable reviews. Thanks for funding and support are due to a Curtin Research and Teaching Fellowship, Australian Research Council Discovery DP1090475 to Evans, and Core to Crust Fluid Systems funding to McCuaig and Hagemann. This is TiGeR publication number 423.

REFERENCES CITED

Angerer, T., and Hagemann, S.G., 2010, The BIF-hosted high-grade iron ore deposits in the Archean Koolyanobbing Greenstone Belt, Western Australia: Structural control on synorogenic- and weathering-related magnetite-, hematite-, and goethite-rich iron ore: Economic Geology and the Bulletin of the Society of Economic Geologists, v. 105, p. 917–945, doi:10.2113/gsecongeo.105.5.917.

Barley, M.E., Pickard, A.L., Hagemann, S.G., and Folkert, S.L., 1999, Hydrothermal origin of the 2 billion year old Mount Tom Pirce giant irohn ore deposit, Hamersley province, Western Australia: Mineralium Deposita, v. 34, p. 784–789.

Bekker, A., and Holland, H.D., 2012, Oxygen overshoot and recovery during the early Paleoproterozoic: Earth and Planetary Science Letters, v. 317, p. 295–304, doi:10.1016/j.epsl.2011.12.012.

Bekker, A., Slack, J.F., Planavsky, N., Krapez, B., Hofmann, A., Konhauser, K.O., and Rouxel, O.J., 2010, Iron formation: The sedimentary product of a complex interplay among mantle, tectonic, oceanic, and biospheric processes:

Economic Geology and the Bulletin of the Society of Economic Geologists, v. 105, p. 467–508, doi:10.2113/gsecongeo.105.3.467.

Beukes, N.J., and Gutzmer, J., 2008, Origin and paleoenvironmental significance of major iron formations at the Archean-Paleoproterozoic boundary, *in* Hagemann, S., et al., eds., Banded iron formation–related high-grade iron ore: Reviews in Economic Geology Volume 15: Littleton, Colorado, Society of Economic Geologists, p. 5–47.

Barnes, S.J., and Hoatson, D.M., 1994, The Munni-Munni Complex, Western Australia—Stratigraphy, structure and petrogenesis: Journal of Petrology, v. 35, p. 715–751, doi:10.1093/petrology/35.3.715.

Brown, M.C., Oliver, N.H.S., and Dickens, G.R., 2004, Veins and hydrothermal fluid flow in the Mt. Whaleback Iron Ore District, eastern Hamersley Province, Western Australia: Precambrian Research, v. 128, p. 441–474, doi:10.1016/j.precamres.2003.09.013.

Busey, R.H., and Mesmer, R.E., 1977, Ionization equilibria of silicic acid and polysilicate formation in aqueous sodium chloride solutions to 300 °C: Inorganic Chemistry, v. 16, p. 2444–2450, doi:10.1021/ic50176a004.

Dalstra, H.J., and Rosiere, C.A., 2004, Structural controls on high-grade iron ores hosted by banded iron formation: A global perspective, *in* Hagemann, S., et al., eds., Banded iron formation-related high-grade iron ore: Littleton, Colorado, Society of Economic Geologists, v. 15, p. 73-106.

Davy, R., 1975, A geochemical study of a dolomite-BIF transition in the lower part of the Hamersley Group: Geological Survey of Western Australia Annual Report, v. 1974, p. 88–101.

El Tabakh, M., Grey, K., Pirajno, F., and Schreiber, B.C., 1999, Pseudomorphs after evaporitic minerals interbedded with 2.2 Ga stromatolites of the Yerrida basin, Western Australia: Origin and significance: Geology, v. 27, p. 871–874, doi:10.1130/0091-7613(1999)027<0871:PAEMIW>2.3.CO;2.

Evans, K.A., and Bickle, M.J., 1999, Determination of time-integrated metamorphic fluid fluxes from the reaction progress of multivariant assemblages: Contributions to Mineralogy and Petrology, v. 134, p. 277–293, doi:10.1007/s004100050484.

Evans, K.A., Gandy, C.J., and Banwart, S.A., 2003, Mineralogical, numerical and analytical studies of the coupled oxidation of pyrite and coal: Mineralogical Magazine, v. 67, p. 381–398, doi:10.1180/0026461036720107.

Farquhar, J., Wu, N.P., Canfield, D.E., and Oduro, H., 2010, Connections between sulfur cycle evolution, sulfur isotopes, sediments, and base metal sulfide deposits: Economic Geology and the Bulletin of the Society of Economic Geologists, v. 105, p. 509–533, doi:10.2113/gsecongeo.105.3.509.

Gleeson, S.A., and Yardley, B.W.D., 2003, Surface-derived fluids in basement rocks; Inferences from palaeo-hydrothermal systems: Journal of Geochemical Exploration, v. 78, p. 61–65.

Gonzalez-Alvarez, I., and Kerrich, R., 2011, Trace element mobility in dolomitic argillites of the Mesoproterozoic Belt-Purcell Supergroup, western North America: Geochimica et Cosmochimica Acta, v. 75, p. 1733–1756, doi:10.1016/j.gca.2011.01.006.

Gosselin, D.C., Sibray, S., and Ayers, J., 1994, Geochemistry of K-rich alkaline lakes, western Sandhills, Nebraska, USA: Geochimica et Cosmochimica Acta, v. 58, p. 1403–1418, doi:10.1016/0016-7037(94)90545-2.

Gutzmer, J., Mukhopadhyay, J., Beukes, N.J., Pack, A., Hayashi, K., and Sharp, Z.D., 2006, Oxygen isotope composition of hematite and genesis of high-grade BIF-hosted iron ores, *in* Kesler, S.E., and Ohmoto, H., eds., Evolution of early Earth's atmosphere, hydrosphere, and biosphere—Constraints from ore deposits: Geological Society of America Memoir 198, p. 257–268, doi:10.1130/2006.1198(15).

Hagemann, S.G., Barley, M.E., and Folkert, S.L., 1999, A hydrothermal origin for the giant BIF-hosted Tom Price iron ore deposit, *in* Stanley, C.J., ed., Mineral deposits, processes to processing: Rotterdam, Balkema, p. 41–44.

Holland, H.D., 2005, Sedimentary mineral deposits and the evolution of Earth's near-surface environments: Economic Geology and the Bulletin of the Society of Economic Geologists, v. 100, p. 1489–1509, doi:10.2113/gsecongeo.100.8.1489.

Isley, A.E., and Abbott, D.H., 1999, Plume-related mafic volcanism and the deposition of banded iron formation: Journal of Geophysical Research, v. 104, p. 15,461–15,477, doi:10.1029/1999JB900066.

Jones, G.D., Whitaker, F.F., Smart, P.L., and Sanford, W.E., 2002, Fate of reflux brines in carbonate platforms: Geology, v. 30, p. 371–374, doi:10.1130/0091-7613(2002)030<0371:FORBIC>2.0.CO;2.

Klein, C., and Beukes, N.J., 1993, Sedimentology and geochemistry of the glaciogenic Late Proterozoic Rapitan Iron Formation in Canada: Economic Geology, v. 88, p. 542–565, doi:10.2113/gsecongeo. 88.3.542.

Leach, D.L., Bradley, D.C., Huston, D., Pisarevsky, S.A., Taylor, R.D., and Gardoll, S.J., 2010, Sediment-hosted lead-zinc deposits in Earth history: Economic Geology and the Bulletin of the Society of Economic Geologists, v. 105, p. 593–625, doi:10.2113/gsecongeo.105.3.593.

Li, Z.X., 2000, Palaeomagnetic evidence for unification of the North and West Australian cratons by ca. 1.7 Ga: New results from the Kimberley Basin of northwestern Australia: Geophysical Journal International, v. 142, p. 173–180, doi:10.1046/j.1365-246x.2000.00143.x.

Manning, C.E., 1994, The solubility of quartz in H_2O in the lower crust and upper mantle: Geochimica et Cosmochimica Acta, v. 58, p. 4831–4839, doi:10.1016/0016-7037(94)90214-3.

Morris, R.C., Thornber, M.R., and Ewers, W.E., 1980, Deep-seaterd iron ores from banded iron formation: Nature, v. 288, p. 250–252.

McLellan, J.G., Oliver, N.H.S., and Schaubs, P.M., 2004, Fluid flow in extensional environments; numerical modelling with an application to Hamersley iron ores: Journal of Structural Geology, v. 26, p. 1157–1171, doi:10.1016/j.jsg.2003.11.015.

Mukhopadhyay, J., Gutzmer, J., Beukes, N.J., and Bhattacharya, H.N., 2008, Geology and genesis of the major banded iron formation-hosted high-grade iron ore deposits of India, *in* Hagemann, S., et al., eds., Banded iron formation–related high-grade iron ore: Reviews in Economic Geology Volume 15: Littleton, Colorado, Society of Economic Geologists, p. 291–316.

Oliver, N.H.S. and Dickens, G.R., 1999, Hematite ores of Australia formed by syntectonic heated meteoric fluids, *in* Stanley, C.J, et al., eds., Mineral Deposits: Processes to Processing: Rotterdam, Balkema, p. 889–892.

Rasmussen, B., Fletcher, I.R., Muhling, J.R., Thorne, W.S., and Broadbent, G.C., 2007, Prolonged history of episodic fluid flow in giant hematite ore bodies: Evidence from in situ U-Pb geochronology of hydrothermal xenotime: Earth and Planetary Science Letters, v. 258, p. 249–259, doi:10.1016/j.epsl.2007.03.033.

Rosiere, C.A., Spier, C.A., Rios, F.J., and Suckau, V.E., 2008, The Itabirites of the Quadrilatero Ferrifero and related high-grade ion ore deposits: An overview, *in* Hagemann, S., et al., eds., Banded iron formation–related high-grade iron ore: Reviews in Economic Geology Volume 15: Littleton, Colorado, Society of Economic Geologists, p. 223–254.

Shmulovich, K.I., Yardley, B.W., and Graham, C.M., 2006, The solubility of quartz in crustal fluids: Experiments and general equations for salt solutions and H_2O-CO_2 mixtures at 400°–800°C and 0.1–0.9 GPa: Geofluids, v. 6, p. 154–167, doi:10.1111/j.1468-8123.2006.00140.x.

Shvarov, Y., and Bastrakov, E., 1999, HCh: A software package for geochemical equilibrium modelling. User's guide: Canberra, Australian Geological Survey Organisation, https://www.ga.gov.au/products/servlet/controller?event=GEOCAT_DETAILS&catno=25473.

Taylor, D., Dalstra, H.J., Harding, A.E., Broadbent, G.C., and Barley, M.E., 2001, Genesis of high-grade hematite orebodies of the Hamersley province, Western Australia: Economic Geology and the Bulletin of the Society of Economic Geologists, v. 96, p. 837–873, doi:10.2113/gsecongeo.96.4.837.

Thorne, A.M., and Tyler, I.M., 1997, Mount Bruce, Western Australia., 1:250 000 geological series explanatory notes., Volume Sheet SF 50-11.

Thorne, W.S., Hagemann, S.G., and Barley, M., 2004, Petrographic and geochemical evidence for hydrothermal evolution of the North Deposit, Mt Tom Price, Western Australia: Mineralium Deposita, v. 39, p. 766–783, doi:10.1007/s00126-004-0444-x.

Thorne, W., Hagemann, S., Webb, A., and Clout, J., 2008, Banded iron formation-related iron ore deposits of the Hamersley Province, Western Australia, *in* Hagemann, S., et al., eds., Banded iron formation–related high-grade iron ore: Reviews in Economic Geology Volume 15: Littleton, Colorado, Society of Economic Geologists, p. 197–221.

Thorne, W., Hagemann, S., Vennemann, T., and Oliver, N., 2009, Oxygen isotope compositions of iron oxides from high-grade BIF-hosted iron ore deposits of the Central Hamersley Province, Western Australia: Constraints on the evolution of hydrothermal fluids: Economic Geology and the Bulletin of the Society of Economic Geologists, v. 104, p. 1019–1035, doi:10.2113/gsecongeo.104.7.1019.

Thorne, W., Hagemann, S., and Banks, D., 2010, Halogen and cation constraints on the origin of hydrothermal fluids forming high-grade iron ore deposits in the Hamersley Province, Western Australia: Smart Science for Exploration and Mining, v. 1–2, p. 582–584.

Young, G.M., 1976, Iron-formation and glaciogenic rocks of the Rapitan Group, Northwest Territories, Canada: Precambrian Research, v. 3, p. 137–158, doi:10.1016/0301-9268(76)90030-9.

Manuscript received 27 January 2012
Revised manuscript received 2 August 2012
Manuscript accepted 18 August 2012

Printed in USA